JOURNAL OF GEOPHYSICAL RESEARCH: OCEANS, VOL. 118, 5238–5250, doi:10.1002/jgrc.20398, 2013

Extreme air-sea interactions in the Gulf of Trieste (North Adriatic) during the strong Bora event in winter 2012

F. Raicich,[1] V. Malačič,[2] M. Celio,[3] D. Giaiotti,[3] C. Cantoni,[1] R. R. Colucci,[1] B. Čermelj,[2] and A. Pucillo[3]

Received 3 June 2013; revised 11 September 2013; accepted 12 September 2013; published 11 October 2013.

[1] From late January to mid-February 2012 the Gulf of Trieste (North Adriatic Sea) was affected by a severe winter weather event characterized by cold air and strong northeasterly wind (Bora). The atmospheric forcing caused large surface heat fluxes which produced remarkable effects on the gulf, particularly the production of a very cold and dense water mass. Temperatures as low as 4°C were observed in the deepest part of the gulf, similar to that which was observed in winter 1929, which was probably the most severe winter in the region over more than a century. The density anomaly attained values up to 30.58 kg m^{-3}, even greater than in 1929. Surface heat fluxes were estimated using bulk formulas and the meteorological and marine observations available at three stations. Mean daily heat losses exceeded 1000 W m^{-2}. A comparison of this event with similar past events was made using proxy heat fluxes, available since 1978, to account for the air-sea interactions and using temperature and salinity observations, performed since 1996, to account for the effect of heat fluxes on ocean properties. The 2012 Bora episode turned out to be the most severe event of this kind in the Gulf of Trieste for at least the last 35 years and is comparable to that which occurred in 1929. A significant linear correlation was also found between the total surface heat loss and the density increase of the waters in the part of the gulf deeper than 20 m.

Citation: Raicich, F., V. Malačič, M. Celio, D. Giaiotti, C. Cantoni, R. R. Colucci, B. Čermelj, and A. Pucillo (2013), Extreme air-sea interactions in the Gulf of Trieste (North Adriatic) during the strong Bora event in winter 2012, *J. Geophys. Res. Oceans*, *118*, 5238–5250, doi:10.1002/jgrc.20398.

1. Introduction

[2] The Gulf of Trieste represents the northernmost point of the Adriatic Sea and is approximately delimited by a line connecting the towns of Grado and Piran (Figure 1). It is a relatively small gulf of about 20 × 25 km^2 with a maximum depth of 25 m.

[3] As the basin is shallow and semienclosed, the effect of meteorology on the water body is remarkable, determining a large variability in temperature, salinity, and therefore density. On synoptic time scales the area is often subject to bursts of the katabatic northeasterly to easterly wind blowing from the Karst Plateau, named Bora in Italian and burja in Slovenian, which causes coastal upwelling [e.g., *Crisciani and Raicich*, 2004; *Crise et al.*, 2006] and intense air-sea heat fluxes [*Stravisi and Crisciani*, 1986; *Picco*, 1991; *Supić and Orlić*, 1999; *Malačič and Petelin*, 2001]. Ocean properties exhibit marked seasonal variability. At the surface the mean sea temperature for 1991–2003 varies from 9°C in February to 25°C in July and practical salinity from 33 in June to 37 in February; at 10 m depth the temperature range is between 9°C in February and 22°C in July–August, while salinity varies between 37 and 38 in all months, being generally higher in winter [*Malačič et al.*, 2006]. Large interannual and interdecadal near-surface sea temperature variability is also observed in correlation with that of air temperature [*Raicich and Crisciani*, 1999]. Climatological annual precipitation amounts to approximately 1000 mm (1043 mm from *Stravisi and Crisciani* [1986]; 973 mm from 1981 to 2010 data, available from the CNR-ISMAR archives), with the minimum in January–February and the maximum in November. The mean river discharge rate into the gulf is estimated to be 114 m^3 s^{-1} over 1998–2008, due mainly to the Isonzo and Timavo rivers [*Cozzi et al.*, 2012].

[4] The Gulf of Trieste is recognized as a site of shelf dense water formation that contributes to the North Adriatic Deep Water [*Malačič and Petelin*, 2001], which then flows cyclonically along the western Adriatic coast and eventually contributes to the Adriatic Deep Water exiting the basin through the Otranto Strait. The process is typical of the winter season, and it is a result of a negative buoyancy flux mainly induced by heat fluxes at the air-sea interface caused by Bora, which drives relatively cold and dry

[1]National Research Council, Institute of Marine Sciences (CNR-ISMAR), Trieste, Italy.
[2]National Institute of Biology, Marine Biology Station (NIB-MBS), Piran, Slovenia.
[3]Regional Environmental Protection Agency (ARPA FVG), Palmanova, Italy.

Corresponding author: F. Raicich, National Research Council, Institute of Marine Sciences (CNR-ISMAR), viale Romolo Gessi 2, 34123 Trieste, Italy. (fabio.raicich@ts.ismar.cnr.it)

2169-9275/13/10.1002/jgrc.20398

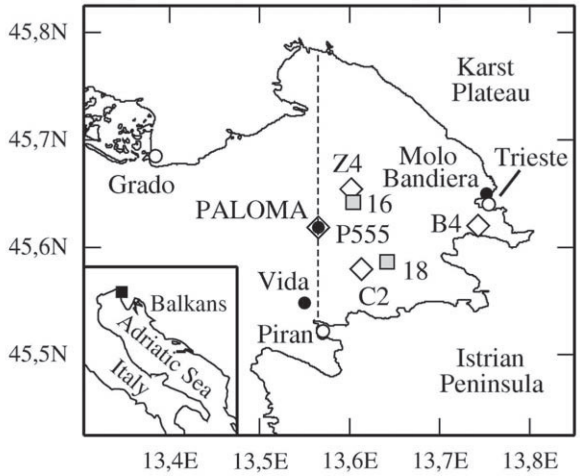

Figure 1. Map of the Gulf of Trieste. The inset shows its position in the Adriatic region. Black dots indicate the stations whose data are analyzed here. The positions of the casts cited in the text are shown by white diamonds (surveys in January and February 2012) and grey squares (surveys in *Vatova* [1934]).

air onto the gulf. Relatively low precipitation and river runoff may determine relatively high salinity, thus preconditioning the water mass. Note that on average, the negative buoyancy flux component due to surface heat loss is largest in autumn, but only in January and February does it prevail over the positive component related to the fresh water inflow from the atmosphere and rivers [*Stravisi and Crisciani*, 1986].

[5] From the end of January to mid-February 2012 a strong and persisting Bora wind affected the Adriatic Sea area and particularly the Gulf of Trieste. Such long-lasting and intense windy weather was the consequence of a persistent atmospheric pressure gradient related to a stable anticyclone extending from Russia westward over central Europe and to generally cyclonic conditions over the Mediterranean Sea. According to Trieste precipitation records (available from CNR-ISMAR archives), this event followed a particularly dry previous quarter (November 2011 to January 2012) with only 31% of the 1981–2010 climatological precipitation amount.

[6] *Mihanović et al*. [2013] studied the 2012 dense water formation in the northern Adriatic shelf and how it has affected the whole Adriatic basin. In this paper we focus on the northernmost site of dense water formation, describing the event and showing how far it was from “normal” winter Bora events. We studied the problem in terms of heat exchanges between sea and atmosphere, and the effect of the event on water column properties, particularly temperature and density. Our analysis will not deal with extreme heat losses in general but only events occurring in winter, defined as January–March. In fact, the largest heat losses in the Gulf of Trieste are observed in autumn, from late October to early December, when frequent strong winds occur together with large sea-air temperature differences [*Stravisi and Crisciani*, 1986; *Supić and Orlić*, 1999; *Rinaldi*, 2006].

[7] Data and methods will be presented in section 2. Section 3 summarizes the results, i.e., the discussion of the 2012 event, its comparison with similar past events as well as the climatology, and a statistical study of the relationship between water density changes and surface heat losses. Conclusions are drawn in section 4.

2. Data and Methods

2.1. Heat Flux Estimates

[8] The total heat flux at the air-sea interface Q is expressed as the sum of the net shortwave radiation flux at the sea surface Q_S, the net longwave radiation flux Q_B, the sensible heat flux Q_H, and the latent heat flux Q_E (all fluxes are positive downward). The heat flux components are estimated by means of the bulk formulas (in SI units) adopted by *Artegiani et al*. [1997] for the Adriatic Sea and outlined in Appendix A. A comparison of different formulations is beyond the scope of this paper; however, further details can be found in *Castellari et al*. [1998].

2.2. Meteorological and Marine Data

2.2.1. Winter 2012

[9] Three stations provide in situ hourly data for surface heat flux estimates, namely, Molo Bandiera, situated on an external pier of Trieste harbor, the mast platform PALOMA (Piattaforma Avanzata Laboratorio Oceanografico Mare Adriatico – Advanced Platform Oceanographic Laboratory Adriatic Sea) located in the center of the Gulf of Trieste, and Vida buoy, approximately 2 km off Piran (Figure 1). All stations are equipped with automatic instruments for data acquisition, logging, and transmission. Molo Bandiera and PALOMA stations are jointly operated by ARPA FVG and CNR-ISMAR; Vida buoy is operated by NIB-MBS. Meteorological data are also available at the ISMAR building located about 500 m from Molo Bandiera station. Table 1 summarizes the stations' characteristics and the availability of parameters. For the heat flux estimates sea temperatures at 2 or 3 m depths are selected to represent near-surface values. The different depths are not considered to be a critical factor since in typical winter conditions the water column is vertically homogeneous. Solar radiation at PALOMA is also used for Vida station where it is not available. At Vida 10 m wind speed (U_{10}) is estimated from the 5 m data according to the power-law relation

$$U_{10} = U_h \left(\frac{10}{h}\right)^{0.13} \tag{1}$$

where $h = 5$ m [*World Meteorological Organization*, 1983]. As the pressure field exhibits large spatial coherency compared to the size of the Gulf of Trieste, ISMAR building atmospheric pressure (reduced to 0°C and mean sea level) is adopted to represent the whole Gulf of Trieste because it is checked every week against indoor mercury barometers. Fractional cloud cover is not observed locally and is taken from the European Centre for Medium-Range Weather Forecasts (ECMWF, MARS archive at http://www.ecmwf.int/); data are available at 00, 06, 12, and 18 h UTC, and each are used to represent a time window from 3.5 h before to 2.5 h after the relevant time.

[10] Additional data come from two CTD (conductivity-temperature-depth) surveys performed in the Gulf of Trieste on 17 January and 14–16 February 2012, which

Table 1. Stations Providing Meteorological and Marine Observations[a]

	Molo Bandiera	PALOMA	Vida	ISMAR Building
Latitude (°N)	45.651	45.618	45.549	45.644
Longitude (°E)	13.753	13.565	13.551	13.754
Meteorological instruments heights (m)				
Atmospheric pressure	10	10	–	11
Air temperature	10	10	5	11
Relative humidity	10	10	5	11
Scalar wind speed	10	10	5	45
Solar radiation	10	10	–	–
Sea temperature probes depths (m)	0.4, 2, 6	3, 15, 24	3	n.a.
Seafloor depth (m)	6	25	22	n.a.

[a]A dash indicates that data are not available; n.a., not applicable.

provide descriptions of the area before and after the event. These data belong to an oceanographic data set for the Gulf of Trieste consisting of observations performed since 1995 by ARPA FVG, NIB-MBS, and the Istituto Nazionale di Oceanografia e Geofisica (INOGS) during institutional monitoring of the regional coastal waters. The data set can be retrieved from http://ms06lxarpa.arpa.fvg.it/mnt/storage/crma/GoT-2012 and in the following, will be referred to as "GoT 1995–2012."

[11] The heat flux estimates are affected by several sources of uncertainty. We can distinguish random, systematic, and environmental data errors. The random error is associated with instrumental sampling and is expected to be extremely small since each hourly value is the mean of thousands of individual measurements. The systematic error is related to instrumental drifts or failures (the use of data from different instruments may fall into this category). In our case, instruments are routinely calibrated, and when possible, further checks were made after the event. This does not apply to cloud cover which is a model product. The environmental error is white noise related to small-scale fluctuations that cause each measurement to be less accurate in representing the environment than would be expected on the basis of the instrumental errors only. In general, it is reasonable to assume that the environmental error prevails over the other error sources. The error on hourly data is here estimated as the standard deviation of the residual fluctuations obtained after removing the daily cycle (time scales longer than 6 h) from the original time series. Since we are interested in the January–February 2012 event, we take into account only the time series from January to March 2012, which includes the conditions before and after the event. As a result, for all stations we adopt absolute environmental errors ε of 0.3°C for air temperature T_a, 0.1°C for near-surface sea temperature T_s, 3% for relative humidity U, 0.3 hPa for atmospheric pressure p_a, and 0.1 for fractional cloud cover C. A relative environmental error η of 12% is adopted for wind speed w. An exception is the solar radiation flux Q_I, for which a 5% error is adopted, corresponding to the measurement accuracy. Details on the heat flux error estimates are included in Appendix B. Note that we do not take into account different bulk formulations, and so this additional source of uncertainty is disregarded.

2.2.2. Multidecadal Time Series

[12] In order to assess the severity of the 2012 event, the heat fluxes of that year should be compared with long-term climatologies and similar previous events. Strictly speaking, such comparisons can only be made if homogeneous time series of meteorological and marine data are available, which in our case, is true only for relatively short periods, specifically 19 years for Molo Bandiera station, 10 years for PALOMA, and 10 years for Vida, all of which, moreover, are affected by gaps.

[13] A way to overcome this limitation is to produce multidecadal time series of proxy heat fluxes from which a climatology can then be derived. We take advantage of the meteorological observations performed at the ISMAR building station and the near-sea surface temperature time series collected in Trieste harbor.

[14] Air temperature, atmospheric pressure, relative humidity, and wind speed have also been measured at the ISMAR building station since summer 1950. Unfortunately, wind data are homogeneous only since summer 1977 because of an anemometer change. Despite the short distance between the ISMAR building and Molo Bandiera the meteorological parameters at the two sites exhibit significant differences in terms of means and daily cycles because of different exposures to wind and the Sun; the ISMAR building is, in fact, partly shielded from Bora by a nearby hill. A comparison made for the 1 January to 31 March 2012 period shows that air temperature at Molo Bandiera is higher than at the ISMAR building by 0.5°C and scalar wind speed is higher by 45%. The same comparison for the 28 January to 12 February event gives 0.6°C and 54%, respectively. Relative humidity is much more difficult to compare because it is measured in a meteorological hut at the ISMAR building and in the open air at Molo Bandiera, and moreover, the two sites are characterized by different ground surface types, i.e., grass and gravel at the ISMAR building and concrete at Molo Bandiera. In January–March 2012 relative humidity is the same (at the unit percent precision) at the two stations, while during the Bora event it is higher at Molo Bandiera by 9%.

[15] A continuous near-surface sea temperature time series is available for Trieste harbor, consisting of one daily measurement performed from 1945 to 2003 with bucket thermometers at about noon at 2 m depth (available from

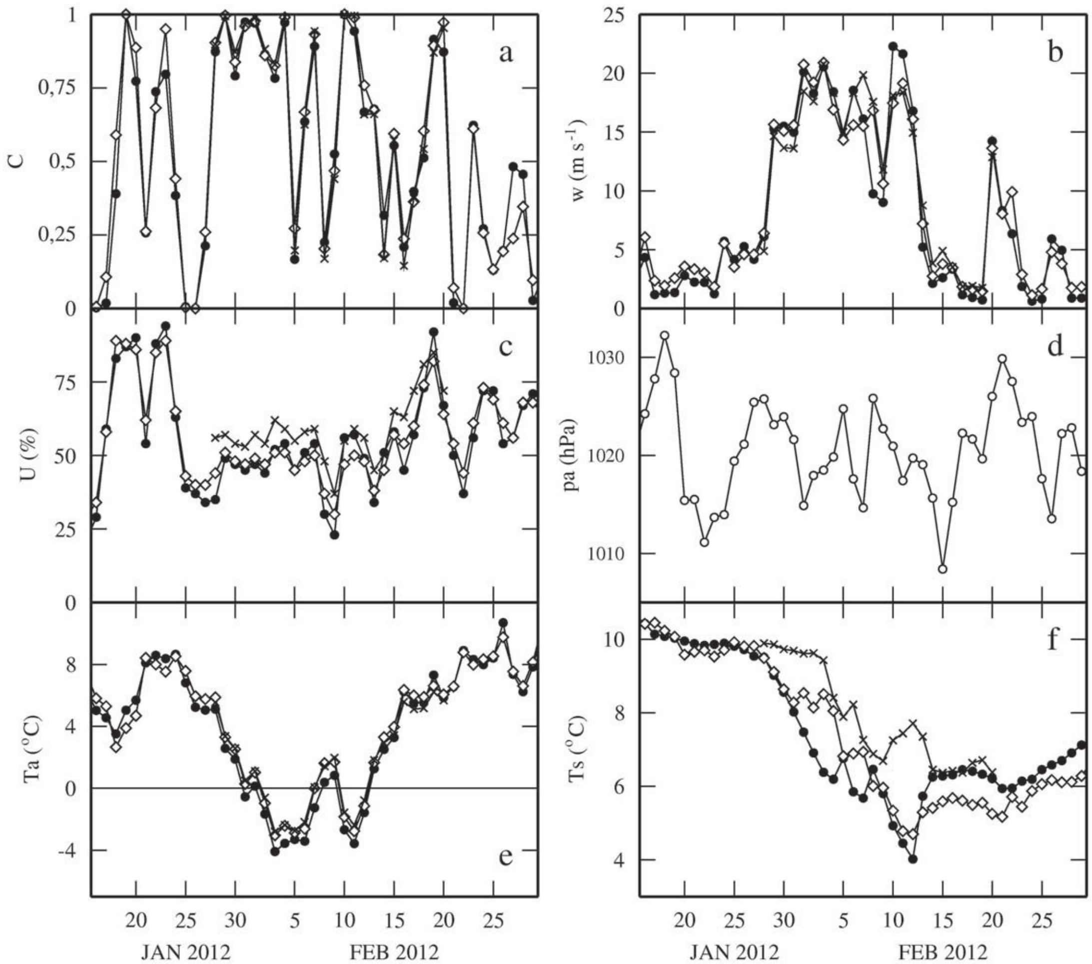

Figure 2. Average daily data of meteorological and marine parameters from 16 January to 29 February 2012 at Molo Bandiera (black dots), PALOMA (white diamonds), and Vida stations (X). (a) Fractional cloud cover C (from ECMWF), (b) scalar wind speed w, (c) relative humidity U, (d) atmospheric pressure p_a (white circles, from the ISMAR building), (e) air temperature T_a, and (f) near-surface sea temperature T_s.

CNR-ISMAR archives). The measurements have always been made within a few hundred meters of Molo Bandiera station, where sea temperature probes have been in operation since 1999. Data for January–March from both sources have been compared for the common period 1999–2003, obtaining a mean difference of $0.06 \pm 0.16°C$ (bucket thermometer data are higher) and a maximum absolute difference of 0.7°C. Therefore, the composite series obtained by merging these two time series can be considered homogeneous for our purposes.

[16] Solar radiation data are not available; therefore, Q_S and Q will not be estimated. Thus, we obtain the time series of proxy daily Q_E, Q_H, and Q_B for the winters from 1978 to 2012, as well as the upward heat flux $Q_U = Q_B + Q_H + Q_E$. The 1978–2011 means will be used as the reference climatology.

3. Results

3.1. The Extreme Bora Event in 2012

[17] The time series of meteorological and marine data for the three stations are displayed in Figure 2. The event of severe winter weather from 28 January to 12 February is characterized by a persistent strong northeasterly wind and relatively dry and cold air. Hourly mean wind speed is often greater than 20 m s^{-1} with peaks on 1, 3, 7, and 10–11 February (Figure 2b). It is apparent that the event consists of two phases, the first showing high spatial coherence of the wind field at the three stations while from 6 February onward differences appear between Molo Bandiera, on the eastern coast, and the two offshore stations PALOMA and Vida. In this second phase a general wind speed decrease is observed from 7 to 9 February when it falls below 10 m s^{-1}, followed by a rapid increase and another peak on 10–11 February. Moreover, wind at Molo Bandiera exhibits more marked fluctuations than at the offshore stations because of the high turbulence induced by the vicinity to the coast and the Karst Plateau. The sudden wind speed drop on 12 February marks the end of the episode. During the entire event relative humidity is around 50% except in the interval of relatively low wind speed on 8–9 February, when it drops to 30% at Vida and less than 20% at PALOMA and Molo Bandiera (Figure 2c). Air temperature exhibits a general decrease at all stations (Molo Bandiera is

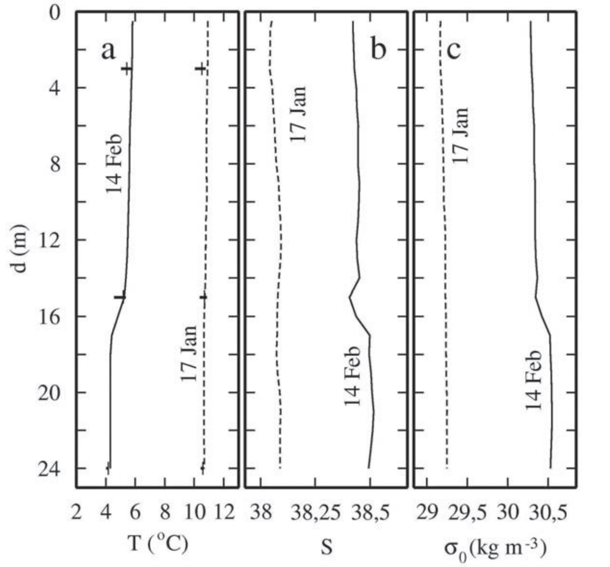

Figure 3. Profiles of (a) temperature, (b) salinity, and (c) potential density anomaly σ_0 at station P555 before (dotted lines) and after (solid lines) the Bora event. Symbols in Figure 3a represent temperature measurements at PALOMA station; the horizontal bars indicate the temperature range of hourly measurements on the relevant day.

slightly colder because of its coastal position) until 3 February, then we observe a steady phase lasting 3 days, an increase between 6 and 9 February from approximately -3 to $+2$°C, and another sharp cooling down to -3°C on 11 February. The last two fluctuations correspond to the wind weakening and the subsequent abrupt strengthening (Figure 2e). Air temperature always remains below the freezing point between 2 and 6 February and between 10 and 12 February. Besides a marked general cooling, the near-surface sea temperature behaves differently at the three stations. At Molo Bandiera the very shallow water column is more sensitive to atmospheric forcing changes and exhibits a slight warming when wind speed decreases, while at PALOMA sea temperature decreases throughout the event, more slowly until 4 February and more rapidly afterward (Figure 2f). At Vida the behavior is similar to PALOMA except that after 8 February, during the last phase of the event, no further cooling is observed. The warming on 9–12 February is likely related to the advection of warmer waters, but there is a lack of data to confirm this statement. Nonetheless, acoustic Doppler current profiler data measured below Vida clearly show that around 11 February, a northward current extends from 4 m depth to the seafloor and may bring warmer waters from the south. By contrast, the lowest temperatures at PALOMA and Molo Bandiera between 4 and 5°C are observed at the end of the event when a local temperature maximum of about 7.5°C is reached at Vida.

[18] The water column properties of the gulf are affected to a large extent by the Bora event. Figure 3 shows temperature, salinity, and potential density anomaly (σ_0) profiles collected on 17 January, before the event, and 14 February, after the event, at station P555, adjacent to PALOMA (Figure 1); temperatures measured on the same days at PALOMA at 3, 15, and 24 m depths are consistent with the profile data (Figure 3). As a result of the Bora event, the average temperature of the surface layer (1–5 m depth) decreases from 10.89 to 5.76°C, salinity increases from 38.05 to 38.43, and σ_0 increases from 29.17 to 30.30 kg m^{-3}; in the bottom layer (20–24 m) average temperature decreases from 10.66 to 4.31°C, salinity increases from 38.09 to 38.51, and σ_0 increases from 29.25 to 30.54 kg m^{-3}.

[19] From the continuous observations at PALOMA station, sea temperature turns out to be vertically homogeneous during the event. By contrast, after Bora has ceased to blow, cold and dense waters formed on the shallow (less than 10 m deep) northern shelf sink into the deepest part of the gulf around PALOMA station. This situation is illustrated by the meridional cross sections along the dashed segment in Figure 1, obtained from a spatial objective analysis of the profiles measured during the survey performed on 14 February (Figure 4). On the northern slope σ_0 exceeds 30.4 kg m^{-3} (Figure 4a), and temperature is lower than 5°C, reaching even 3.8°C in the shallowest area (Figure 4b). The cold water mass remains in the deep gulf from 13 to 20 February, exhibiting a slight warming trend, while near the surface the water column becomes warmer by about 1.5°C (Figure 5). Another windy period on 20–23 February destroys the vertical stratification. The average vertical temperature, computed from the observations at 3, 15, and 24 m, exhibits a slight increasing trend after 13 February, consistent with that of the bottom layer temperature, and no abrupt change is observed when wind starts

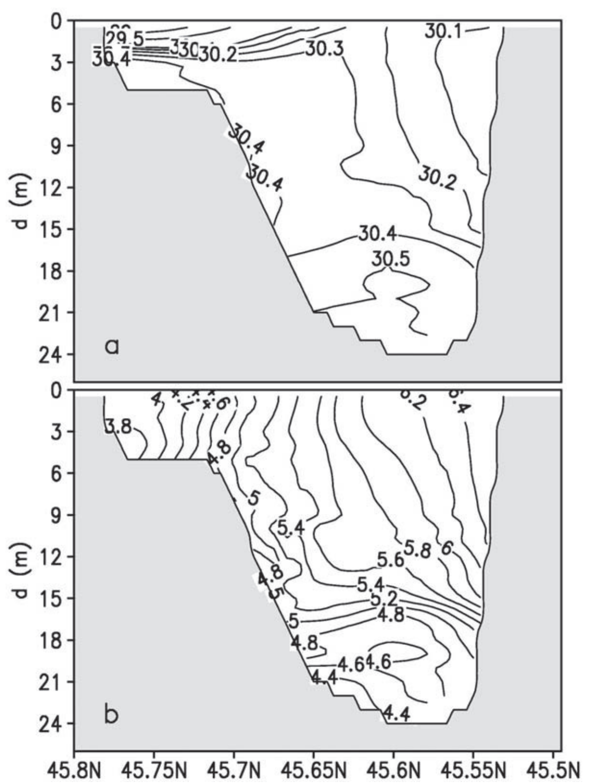

Figure 4. Meridional cross sections of (a) potential density anomaly and (b) temperature from data observed on 14 February 2012 along the dashed segment in Figure 1.

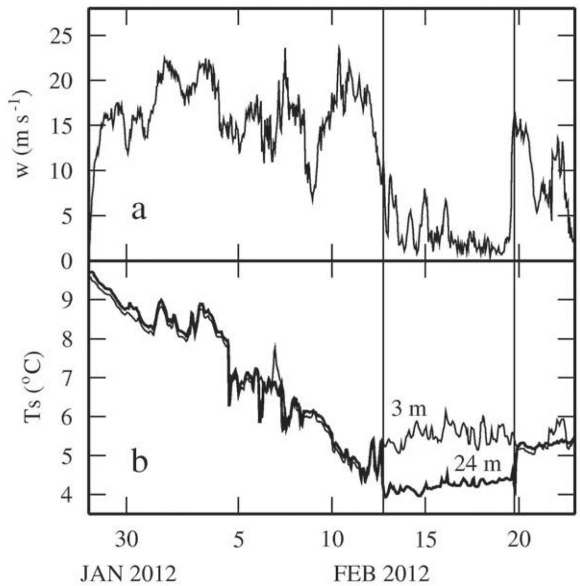

Figure 5. PALOMA station hourly data from 28 January to 23 February 2012. (a) Wind speed w and (b) sea temperature T_s at 3 m depth (thin line) and 24 m depth (thick line).

blowing on 20 February (not shown). This means that in the area near PALOMA on that day, wind mainly induced a vertical heat redistribution by convection and forced vertical mixing, rather than the advection of warmer waters.

[20] At 15 m depth, temperature exhibits fluctuations with the inertial period of 16.7 h (not shown), and an amplitude around 0.2°C, as revealed by Fourier analysis. This phenomenon deserves further attention.

[21] Table 2 summarizes hourly and daily means and extremes observed at the three stations during the Bora event for the variables that are most relevant to heat flux estimates, namely, air temperature, sea temperature, sea-air temperature difference, and scalar wind speed. The time series of mean daily heat flux components and totals are displayed in Figure 6. The event is characterized essentially by large sensible and latent heat fluxes, which affect the upward heat flux Q_U (sum of Q_B, Q_H, and Q_E) and the net heat flux Q. Means and extremes of the heat flux components during the event are summarized in Table 3. From Q_E we estimate mean evaporation rates (equation (A15)) of 12.8, 13.3, and 14.0 mm d^{-1} at Molo Bandiera, PALOMA and Vida, respectively, corresponding to total evaporation of 205, 213, and 224 mm throughout the Bora event.

[22] An estimate of the density increase due to evaporation helps in estimating the shares between the increase of density due to cooling and that due to evaporation. Let us take the PALOMA station estimate of $h_e = 213$ mm for the evaporation over the whole Bora event. During evaporation the mass of salt inside the sea remains constant, which also holds for the area around PALOMA. Since during the windy conditions the water column is vertically homogeneous, the conservation of salt can be written as

$$S_0 H = S(H - h_e) \tag{2}$$

where S_0 and S are the salinities before and after the Bora event, respectively, and H is the water depth (25 m at PALOMA). From Figure 3b the vertically averaged salinity before the event is $S_0 = 38.07$; therefore,

$$S = S_0\left(1 - \frac{h_e}{H}\right)^{-1} = 1.009 S_0 = 38.40 \tag{3}$$

which despite the simplicity of the approach, is quite consistent with the vertically averaged salinity of 38.46 observed after the event (Figure 3b).

[23] We may also reasonably approximate, in this simplistic view, that relative density changes depend linearly on salinity and temperature changes as

$$\frac{\Delta\rho_0}{\rho_0} = -\alpha\Delta T + \beta\Delta S \tag{4}$$

[24] The ratio between $\alpha\Delta T$ and $\beta\Delta S$ measures the importance of density increase due to cooling with respect to its increase by evaporation. Let us take for α (thermal expansion coefficient) and β (saline contraction coefficient) the values for $T = 7.97$°C and $S = 38.25$, which are the average temperature and salinity before and after the event (Figures 3a and 3b): $\alpha = 1.54 \times 10^{-4}$°C^{-1} and $\beta = 7.64 \times 10^{-4}$. Taking the observed mean changes of temperature $\Delta T = -5.60$°C and salinity $\Delta S = 0.39$, the computed relative density change is 1.16 kg m^{-3} while from observation it is 1.09 kg m^{-3}. The ratio $\alpha\Delta T/\beta\Delta S = 2.89$, meaning that the density increase due to forced cooling is almost three times larger than that due to evaporation, which itself, is far from being negligible.

Table 2. Means and Daily and Hourly Extremes Recorded During the 28 January to 12 February 2012 Period for Selected Parameters[a]

Site	Data Type	T_a (°C) (Minimum)	T_s (°C) (Minimum)	$T_s - T_a$ (°C) (Maximum)	w (m s^{-1}) (Maximum)
B	Mean	−0.9	6.6	7.6	16.1
	Daily	−4.1 3 Feb	4.0 12 Feb	10.5 3 Feb	22.3 10 Feb
	Hourly	−4.8 4 Feb (05)	3.8 12 Feb (20)	10.9 3 Feb (07)	27.2 11 Feb (01)
P	Mean	−0.1	7.3	7.4	16.0
	Daily	−3.0 3 Feb	4.7 12 Feb	11.5 3 Feb	20.9 3 Feb
	Hourly	−4.1 6 Feb (07)	4.3 12 Feb (07)	12.0 3 Feb (09)	23.6 8 Feb (00)
V	Mean	0.1	8.5	8.4	16.0
	Daily	−2.8 3 Feb	7.2 10 Feb	12.2 3 Feb	20.8 3 Feb
	Hourly	−3.5 6 Feb (08)	6.2 7 Feb (15)	12.8 3 Feb (05)	25.9 7 Feb (19)

[a]B, Molo Bandiera station; P, PALOMA station; V, Vida station. UTC hour in brackets.

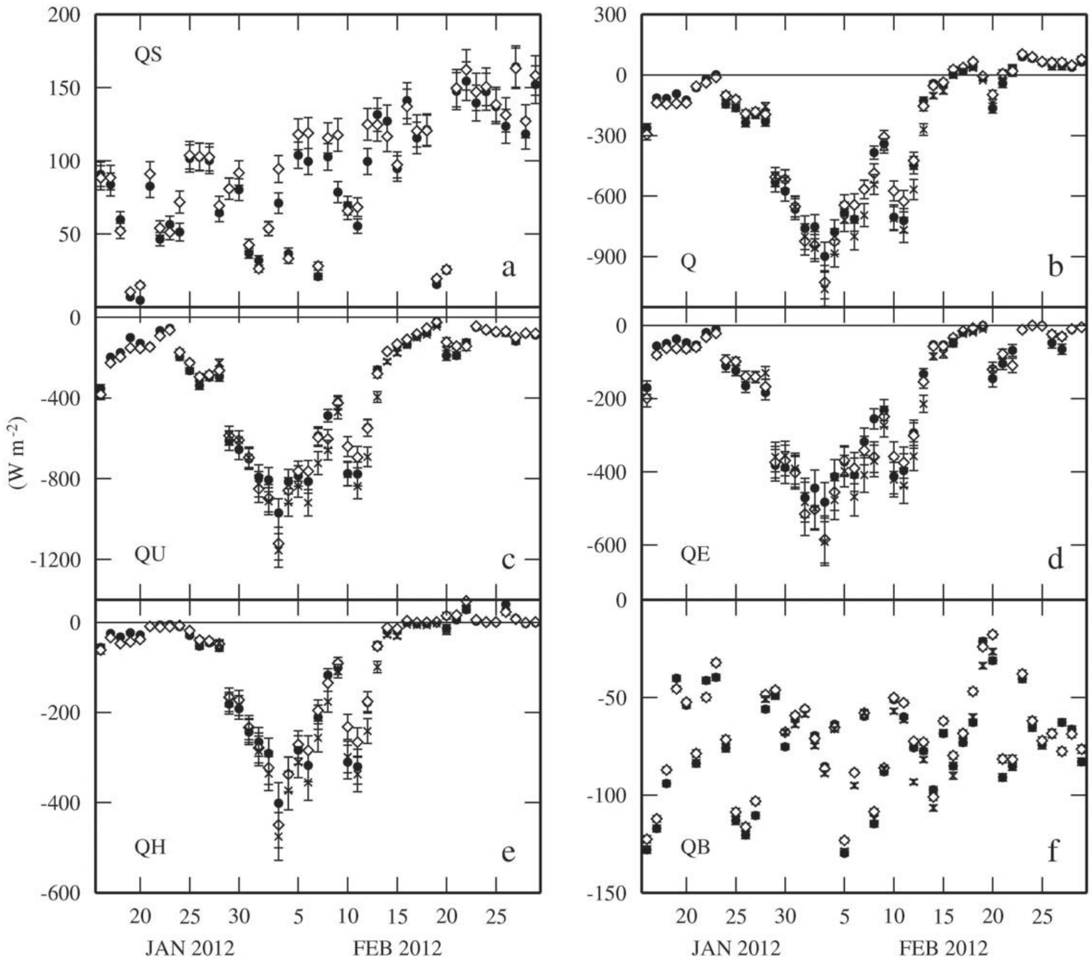

Figure 6. Average daily heat flux components and errors from 16 January to 29 February 2012 from data at Molo Bandiera (black dots), PALOMA (white diamonds), and Vida stations (X). (a) Solar heat flux Q_S, (b) total heat flux Q, (c) net upward heat flux Q_U, (d) latent heat flux Q_E, (e) sensible heat flux Q_H, and (f) net longwave heat flux Q_B.

3.2. Comparison With Similar Previous Events

[25] We compare the 2012 event with similar past episodes. The events are studied in terms of overall atmosphere-sea interactions and their effects on the sea water body, i.e., the surface heat fluxes and water column properties, instead of looking at individual atmospheric and marine parameters.

3.2.1. Surface Heat Fluxes

[26] The persistent strong wind and low air and sea temperatures suggest that the heat fluxes in winter 2012 are remarkable, but it is difficult to find similar detailed analyses of heat fluxes in the Gulf of Trieste in previous strong Bora events.

[27] As an example, we consider an event which occurred in February 2003 studied by *Dorman et al*. [2006]

Table 3. Means and Daily Extremes During the 28 January to 12 February 2012 Period for Heat Flux Components[a]

Site	Data type	Q (W m^{-2})	Q_U (W m^{-2})	Q_S (W m^{-2})	Q_E (W m^{-2})	Q_H (W m^{-2})	Q_B (W m^{-2})
B	Mean	−610	−678	68	−366	−238	−74
	Extreme	−905	−976	104	−483	−402	−134
	Date	3 Feb	3 Feb	5 Feb	3 Feb	3 Feb	5 Feb
P	Mean	−604	−682	78	−382	−229	−71
	Extreme	−1032	−1126	125	−585	−450	−129
	Date	3 Feb	3 Feb	12 Feb	3 Feb	3 Feb	5 Feb
V	Mean	−662	−740	78	−402	−263	−76
	Extreme	−1066	−1161	125	−591	−476	−134
	Date	3 Feb	3 Feb	12 Feb	3 Feb	3 Feb	5 Feb

[a]B, Molo Bandiera station; P, PALOMA station; V, Vida station.

from open sea observations and the Coupled Ocean/Atmosphere Mesoscale Prediction System (COAMPS) data that cover the northern and central Adriatic. Unfortunately, a comparison for the Gulf of Trieste is not possible from direct observations because the area is only covered by COAMPS data [*Dorman et al.*, 2006, Figure 15]. The authors report a mean February total heat flux Q between -300 and -400 W m^{-2} which when also considering that different formulas were used for the heat budget estimate, appears to be very different from the estimate of -147 W m^{-2} made from observations at Molo Bandiera and the bulk formulas used in this paper (Appendix A). A probable reason for this discrepancy is that the sea-air temperature difference from COAMPS is too large, specifically about 8°C [*Dorman et al.*, 2006, Figure 3], while we find only 2.5°C. In general, as the authors state, COAMPS overestimates heat losses at coastal and near-coastal stations and underestimate them in the middle of the northern Adriatic basin.

[28] Mean heat flux estimates for February 2003 are also available from *Rinaldi* [2006], who used the meteorological data from the ECMWF. As a result (Q, Q_S, Q_E, Q_H, Q_B) = (−198, 104, −130, −65, −107) W m^{-2}, to be compared with our estimates of (−147, 107, −125, −41, −89) W m^{-2}, respectively. Differences can partly be explained because of the use of ECMWF skin sea temperature instead of near-sea surface temperature, which are essentially equal only during a strong Bora, when the surface part of the water column is vertically homogeneous.

3.2.2. Ocean Properties

[29] Figure 7 shows average temperatures, salinities, and σ_0 for depths greater than 20 m, obtained during surveys performed in January and February in the Gulf of Trieste from 1996 to 2012 and extracted from the "GoT 1995–2012" data set; data for 2012 are highlighted by boxes. The analysis is limited to the bottom waters since they allow us to observe the air-sea interaction signal, by "storing" it much longer than the waters near the surface. In January 2012 the deep water conditions were characterized by $T = 10.41$°C, $S = 37.86$, and $\sigma_0 = 29.11$ kg m^{-3}, corresponding to +0.66°C, −0.01 and −0.12 kg m^{-3}, relative to the 1996–2011 January averages, respectively, whereas in February $T = 4.55$°C, $S = 38.48$, and $\sigma_0 = 30.49$ kg m^{-3}, i.e., −4.03°C, +0.60 and +1.05 kg m^{-3} with respect to the 1996–2011 February averages.

[30] It turns out that since 1996 temperature has never been as low and σ_0 as high as in 2012, and that such large changes of −5.86°C in temperature and +1.38 kg m^{-3} in σ_0 have never been observed in the deep part of the Gulf of Trieste.

[31] The period covered by the above-mentioned surveys represents only the last 16 years, and it is therefore quite short. According to the meteorological time series recorded in the region, several severe winter weather events occurred in the past, probably the most famous being in February 1929 when extremely low air temperatures affected the area, such as −14°C in Trieste and −12°C in Rovinj, on the west coast of the Istrian Peninsula [*Vatova*, 1934]. Oceanographic data were collected in the northern Adriatic, including the Gulf of Trieste, shortly after that event, and this allows us to compare it with the event of 2012 on the basis of water column properties. On 11–12 March 1929, 1 month after the cold spell climax and 1 week after another Bora event, the Italian-German Institute for Marine Biology of Rovinj carried out an oceanographic survey in which the temperature was found to be as low as 3.95°C at 22 m depth at station 18 and 4.00°C at 21.5 m at station 16 (Figure 1) [*Vatova*, 1934].

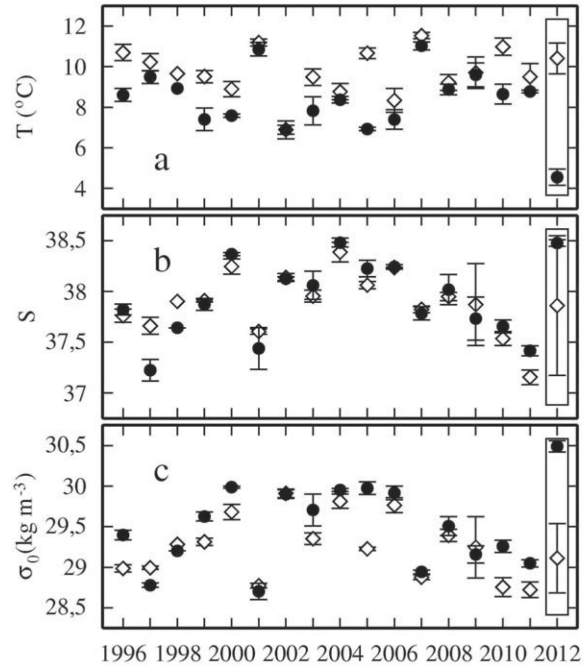

Figure 7. Average (a) temperature T, (b) salinity S, and (c) potential density anomaly σ_0 and respective errors for the part of the Gulf of Trieste deeper than 20 m in January (white diamonds) and February (black dots) from 1996 to 2012.

[32] The values of temperature, salinity, and σ_0 found on 14–16 February 2012, 2 days after the end of the event, at stations C2, P555, and Z4, are compared in Table 4 with those observed in 1929 at stations 16 and 18 [*Vatova*, 1934]. The comparison is made for stations in the deepest part of the Gulf of Trieste, where bottom depth exceeds 20 m, and for the depths reported by Vatova. It must be approached with caution since we do not know the performance capability (calibration, accuracy) of the instruments and analyses of 1929. For comparison with modern data, the σ_0 values in Table 4 have been recalculated from Vatova's temperatures and salinities according to the UNESCO International Equation of State (IES 80), as described in *Fofonoff* [1985], while the original values reported in *Vatova* [1934] are higher by 0.01–0.03 kg m^{-3}. It turns out that temperature and salinity in 2012 are both higher than in 1929 and their combined effect on density determines σ_0 values that are not very different in the two events except at 22 m where σ_0 is clearly higher in 2012. The maximum σ_0 was observed near the bottom (18 m depth) at station B4 (Figure 1) with 30.58 kg m^{-3}, representing the highest value ever recorded in the Gulf of Trieste. Continuous temperature observations made at PALOMA, whose position almost coincides with station P555, show that at 24 m depth water temperature reached

Table 4. Comparison of Sea Water Properties Observed in the Gulf of Trieste in 1929 and 2012[a]

	T (°C)		S		σ_0 (kg m^{-3})	
Depth (m)	1929	2012	1929	2012	1929	2012
0.5	5.05–5.14	5.82–6.14	35.32–38.03	38.22–38.42	27.92–30.06	30.08–30.28
5	5.00–5.10	5.70–6.09	37.97–38.04	38.22–38.44	30.03–30.08	30.09–30.31
15	3.98–4.00	5.25–5.37	38.15	38.33–38.41	30.29–30.30	30.27–30.35
22	3.95–4.00	4.17–4.48	38.15–38.17	38.46–38.51	30.30–30.31	30.50–30.55

[a]Columns report minimum and maximum values observed at stations representative of the deepest part of the gulf. The σ_0 values for 1929 have been recalculated (see text).

the absolute minimum of 3.93°C on 13 February and a secondary minimum of 3.96°C on 15 February, which are very similar to Vatova's observations off Koper.

3.2.3. Multidecadal and Climatological Analyses

[33] In order to check that heat fluxes at the two stations vary coherently, we compared daily heat fluxes from Molo Bandiera data and proxy heat fluxes from ISMAR building data for January–March 2012 obtaining highly significant linear correlation coefficients, i.e., $r = 0.99$ for Q_U, $r = 0.98$ for Q_E, $r > 0.99$ for Q_H, and $r = 0.92$ for Q_B, all of them being significant at $p < 0.001$. This result allows us to use the heat fluxes estimated with ISMAR building data as proxies for the purpose of comparison with events observed in past winters, although we are aware that they do not represent the actual air-sea heat fluxes in the Gulf of Trieste.

[34] Figures 8a–8d display the time series of proxy daily Q_U, Q_E, Q_H, and Q_B in comparison with 1978–2011 climatological daily means and extremes, and Table 5 lists the top 15 daily heat flux components in that period. During most of the Bora event Q_U, Q_E, and Q_H are close to or even surpass the extreme values for each calendar day; moreover, several days of the 2012 event appear in the highest

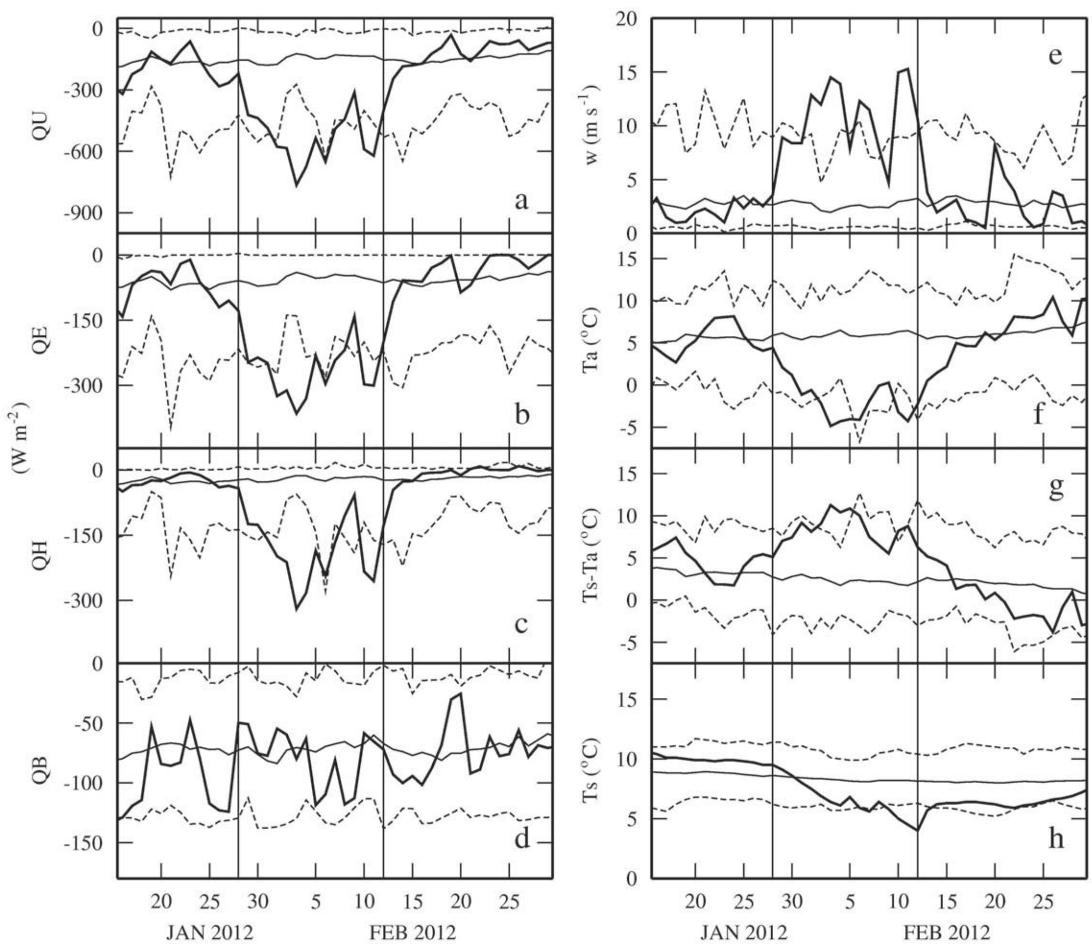

Figure 8. Comparison of daily proxy heat flux components, and average daily parameters used for their estimate, from 16 January to 29 February 2012 (thick solid lines) with 1978–2011 climatological means (thin solid lines) and extremes (dashed lines). (a) Net upward heat flux Q_U, (b) latent heat flux Q_E, (c) sensible heat flux Q_H, (d) net longwave heat flux Q_B, (e) scalar wind speed w, (f) air temperature T_a, (g) difference between sea and air temperatures $T_s - T_a$, and (h) sea temperature T_s.

Table 5. List of the Top 15 Daily Proxy Heat Flux Components in the Winters From 1978 to 2012[a]

	Q_U (W m^{-2})	Date	Q_E (W m^{-2})	Date	Q_H (W m^{-2})	Date	Q_B (W m^{-2})	Date
1	**−765**	**3 Feb 2012**	−396	21 Jan 1992	**−320**	**3 Feb 2012**	−150	6 Jan 1985
2	−740	11 Jan 2003	−387	13 Jan 2001	−283	9 Jan 1985	−148	7 Jan 1985
3	−724	21 Jan 1992	−386	4 Jan 1995	**−283**	**4 Feb 2012**	−147	3 Jan 1979
4	−710	6 Jan 1985	**−365**	**3 Feb 2012**	−279	6 Feb 1991	−146	12 Jan 2003
5	−706	13 Jan 2001	−363	12 Jan 1980	−258	6 Jan 1985	−143	8 Jan 1987
6	−680	9 Jan 1985	−360	11 Jan 2003	**−256**	**11 Feb 2012**	−142	9 Jan 1981
7	−678	4 Jan 1995	**−330**	**4 Feb 2012**	−245	21 Jan 1992	−139	8 Jan 1981
8	**−676**	**4 Feb 2012**	**−325**	**1 Feb 2012**	**−244**	**6 Feb 2012**	−139	11 Jan 2003
9	−654	12 Jan 1980	−318	9 Jan 1985	−242	11 Jan 2003	−139	12 Feb 1985
10	**−650**	**6 Feb 2012**	**−312**	**2 Feb 2012**	**−233**	**10 Feb 2012**	−138	14 Jan 2001
11	−648	14 Feb 1994	−305	14 Feb 1994	−232	9 Jan 2003	−138	30 Jan 1999
12	−634	6 Feb 1991	−303	6 Jan 1985	−226	12 Jan 1980	−138	31 Jan 1987
13	**−622**	**11 Feb 2012**	**−301**	**11 Feb 2012**	−225	5 Jan 1985	−137	25 Jan 2000
14	−616	2 Jan 1993	**−298**	**10 Feb 2012**	−221	14 Feb 1994	−137	1 Feb 1991
15	−613	7 Jan 1985	**−296**	**6 Feb 2012**	−221	7 Jan 1985	−136	30 Jan 1987

[a]Days of 2012 are highlighted in bold.

positions of long-term ranking. In contrast, although Q_B is often lower than the mean, it remains above the lower limit (Figure 8d) and no days of the 2012 event appear in Table 5.

[35] Daily wind speed, air temperature, sea-air temperature difference, and near-surface sea temperature are compared with climatological means and extremes in Figures 8e–8h. Recall that those atmospheric parameters are observed at ISMAR building. Also, these parameters exhibit a significant departure from the means, particularly wind speed which is higher than the climatological maximum during almost the entire event. Air temperature and sea-air temperature difference are close to and sometimes exceed the lower and higher climatological limits, respectively. Despite being higher than the mean at the beginning of the event, sea temperature reaches values close to the climatological minima at the beginning of February and goes below the absolute minimum observed over 1978–2011 by the end of the Bora event.

[36] A remarkable result is obtained by taking into account average heat flux components over 16 days which is the duration of the 2012 Bora episode. Table 6 shows that Q_U, Q_E, and Q_H in 2012 represent the absolute extremes that are much larger (in absolute value) than in the event of December 1984 to January 1985. Again, an exception is Q_B.

[37] From Tables 5 and 6 it can be seen that large heat losses in winter mostly occur in the first half of January and are uncommon in February (i.e., only in 1991, 1994, and 2012). The reason is that early January sometimes exhibits autumn-like conditions that as mentioned earlier, favor the largest heat loss in the Gulf of Trieste [*Stravisi and Crisciani*, 1986; *Supić and Orlić*, 1999].

[38] We find that the event in December 1984 to January 1985 turns out to be the second most severe event after 2012 in terms of heat fluxes. A few CTD profiles (retrieved on 14 March 2013 from the Coriolis data base at www.coriolis.eu.org) were collected in the Gulf of Trieste on 7 February 1985, which is, unfortunately, more than 3 weeks after the end of the event. No other measurements are available for winter 1985. In the deepest area of the gulf bottom temperature was between 7.9 and 8.6°C and salinity was 37.4–37.5, resulting in σ_0 between 29.3 and 29.4 kg m^{-3}. According to the 2 m sea temperature near Molo Bandiera, the minimum temperature was recorded on 17 January at 5.6°C, then the temperature increased to 8.2°C on 8 February and decreased to 6.3°C on 20 February; therefore, the conditions observed on 7 February seem to be representative of a water mass that partly replaced the dense water produced in the first half of January.

[39] As was noted in section 1, dense water formation is a common process in the Gulf of Trieste. Its extent is connected with atmospheric forcing, which determines the amount of newly formed water mass and its density excess with respect to the previous, unperturbed conditions. To study the connection between heat fluxes and density variations, we compare total surface heat fluxes (Q) and density anomaly changes ($\Delta\sigma_0$). The analysis involves the 1996–2012 period, which is covered by the "GoT 1995–2012" data set (see section 2.2.1). The frequency of the oceanographic surveys limits our analysis to a monthly time scale.

Table 6. List of the Top Three 16 day Mean Proxy Heat Flux Components in the Winters From 1978 to 2012[a]

	Q_U (W m^{-2})	Date	Q_E (W m^{-2})	Date	Q_H (W m^{-2})	Date	Q_B (W m^{-2})	Date
1	**−515**	**5 Feb 2012**	**−258**	**4 Feb 2012**	**−178**	**5 Feb 2012**	−117	26 Jan 1991
2	−435	4 Jan 1985	−201	4 Jan 1985	−137	4 Jan 1985	−114	2 Jan 1990
3	−366	2 Jan 1993	−165	2 Jan 2009	−88	2 Jan 2009	−114	28 Jan 1991

[a]Dates indicate the central day of the period; days of 2012 are highlighted in bold.

$\Delta\sigma_0$ represents the difference of monthly mean σ_0 in two consecutive months, namely, σ_0(February) $-$ σ_0(January) or σ_0(March) $-$ σ_0(February), obtained from all observations at depths greater than 20 m; thus, two values are available for each year. The error on σ_0 is represented by the standard deviation of the data sample used for its calculation; the errors on the relevant σ_0 values are then propagated to estimate the error on $\Delta\sigma_0$. Daily Q values are obtained by adding proxy Q_U and solar heat flux Q_S computed from observations according to equation (A2); monthly mean Q values are then obtained from the daily values in the periods 16 January to 15 February and 16 February to 15 March. The errors on Q are obtained from the errors on each component as explained in Appendix B.

[40] Our analysis is limited to the cases when $\Delta\sigma_0 > 0$, that is, denser water has been formed. From January to February this condition occurred every year except in 1997, 1998, 2001, 2002, and 2009, while from February to March it was observed only in 1996, 2001, 2005, and 2011. It turns out that 16 cases satisfy this criterion; they are shown in Figure 9. Under the hypothesis of a linear relationship between $\Delta\sigma_0$ and Q

$$\Delta\sigma_0 = a + bQ \tag{5}$$

regression provides the results summarized in Table 7. The analysis was performed using the Fortran 77 programs in *Press et al*. [1996].

[41] First, we notice that the two linear models, with and without 2012, are consistent with each other, which means that within a one standard deviation confidence limit, $\Delta\sigma_0$ in the extreme case of 2012 can be estimated from the model parameters estimated from the "normal" cases. Second, we can obtain a useful, although crude, estimate of the density anomaly change as a function of heat fluxes. We find that a 1 W m^{-2} total heat loss causes a density increase of approximately $(5 \pm 2) \times 10^{-3}$ kg m^{-3}. This figure is site-specific, but the concept seems applicable to other semienclosed water bodies similar to the Gulf of Trieste.

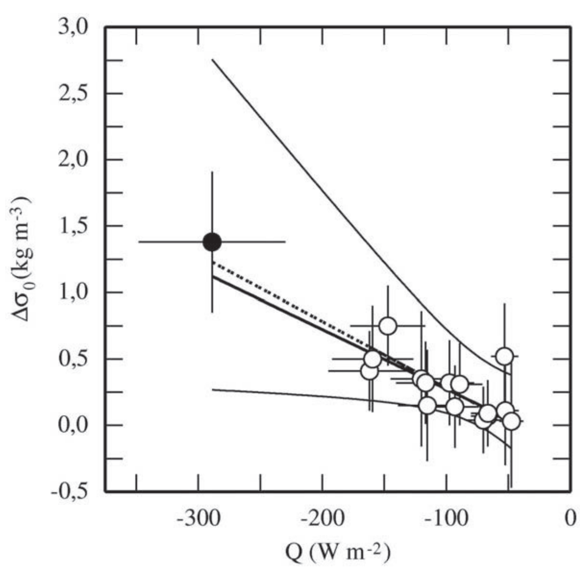

Figure 9. Comparison of mean monthly density anomaly variations ($\Delta\sigma_0$) and mean monthly total heat fluxes (Q) from 1996 to 2012. Error bars on both variables are shown. The 2012 data are indicated by the black dot. The solid lines represent the linear fit for 1996–2011 and related one standard deviation confidence limits. The dashed line represents the 1996–2012 linear fit.

Table 7. Linear Regression Analysis of Monthly Density Anomaly Changes ($\Delta\sigma_0$) and Total Heat Fluxes (Q)[a]

Period	a (kg m^{-3})	b (kg m^{-3}/W m^{-2})	p
1996–2011	-0.2210 ± 0.2049	-0.0050 ± 0.0019	0.7×10^{-3}
1996–2012	-0.1754 ± 0.2454	-0.0045 ± 0.0025	1.4×10^{-3}

[a] a is the intercept, b is the slope, and p represents the probability that the linear relationship occurs by chance and measures the fit quality.

4. Conclusions

[42] This study of the air-sea interactions during winter 2012 reveals that the Bora event from 28 January to 12 February can be considered as an extreme event over the course of several decades in terms of both surface heat fluxes and ocean properties, particularly temperature and density. The most significant feature is the persistence of strong wind which caused extensive evaporation and caused the temperature to drop to values observed only in February 1929, and which created a density even higher than in that month.

[43] It is interesting to note that although the two events mentioned earlier are characterized by similar ocean properties, the atmospheric conditions are quite different during the two winters. In fact, the whole winter of 1929, from the end of December 1928, was much colder and more windy than normal; by contrast, air temperature in 2012 was below normal only during the Bora event, but still much higher than in February 1929 by about 3°C on average and up to 8°C on a daily basis. This suggests that the combination of all the relevant atmospheric and marine parameters must be taken into account to explain the effects of the atmospheric forcing on the water column, while the variations of individual parameters, although useful as indicators of the season's severity, may not be sufficient.

[44] We studied the connection between heat fluxes and density anomaly variations, particularly when the latter are positive, that is, denser water is formed. The analysis illustrated in Figure 9 and Table 7 reveals that although the dense water formation in winter 2012 represents an extreme situation, the magnitude of the observed density change is consistent with the estimate obtained from data from previous winters.

[45] In the comparison with past events a limit to our analysis is the relatively small amount of data that can be used. There are fewer than 20 years of monthly surveys in the gulf and only 35 years of proxy heat fluxes. As a consequence, we cannot make a thorough comparison here with other known past severe Bora episodes as, for instance, that which occurred in February 1956, quoted in *Mihanović et al*. [2013]. The reconstruction of longer homogeneous time series of meteorological and marine data is required to provide more information on this aspect. However, in the context of "present" climate, the January–February 2012

event represents an extreme situation from the viewpoint of dense water formation in the Adriatic, which is also certainly relevant also for the Mediterranean itself.

Appendix A: Bulk Formulas

[46] The total heat flux from the atmosphere to the sea Q can be expressed as

$$Q = Q_S + Q_B + Q_H + Q_E \tag{A1}$$

where Q_S is the net shortwave radiation flux reaching the sea surface, Q_B is the net longwave radiation flux, and Q_H and Q_E are the sensible and latent heat fluxes, respectively. The positive sign indicates heat flux from the atmosphere to the sea.

[47] The shortwave radiation flux Q_S can be written as

$$Q_S = Q_I(1 - \alpha) \tag{A2}$$

where Q_I is directly measured near the sea surface and α is the ocean surface albedo, which depends on atmospheric transmittance and Sun altitude. As a basis, we use monthly climatological values at noon obtained as averages of those proposed by *Payne* [1972] for the North Atlantic at 40°N and 50°N, where the dependence on atmospheric transmittance is averaged out.

[48] The longwave radiation flux Q_B is computed by means of Berliand's formula [*Simpson and Paulson*, 1979]

$$Q_B = -\varepsilon\sigma T_a^4\left(0.39 - 0.05e_a^{1/2}\right)\left(1 - 0.8C^2\right) + 4\varepsilon\sigma T_a^3(T_s - T_a) \tag{A3}$$

where $\varepsilon = 0.97$ is the ocean longwave emissivity, $\sigma = 5.67 \times 10^{-8}$ W m^{-2} K^{-4} is the Stefan–Boltzmann constant, T_s is the sea temperature, T_a is the air temperature, and C is the fractional cloud cover; e_a is the atmospheric vapor pressure, which can be expressed in terms of the saturation vapor pressure e_{sat} and the relative humidity U as

$$e_a = 0.01Ue_{sat}(T_a) \tag{A4}$$

[49] The sensible and latent heat fluxes are written as

$$Q_H = -\rho_M c_H C_p w(T_s - T_a) \tag{A5}$$

$$Q_E = -L(T_s)\rho_M c_E w[e_{sat}(T_s) - 0.01Ue_{sat}(T_a)]0.622p_a^{-1} \tag{A6}$$

where ρ_M is the density of moist air, c_H and c_E are the turbulent exchange coefficients, $C_p = 1.005 \times 10^{-3}$ J kg^{-1} K^{-1} is the specific heat capacity at constant pressure, w is the wind speed, T_s is the sea temperature, T_a is the air temperature, $L(T)$ is the latent heat of vaporization, $e_{sat}(T)$ is the saturation vapor pressure, U is the relative humidity, and p_a is the atmospheric pressure. The number 0.622 represents the ratio between the gas constants for dry air R_d and water vapor R_v. The density of moist air is given by

$$\rho_M = 100\frac{p_a 0.622(1 + r_w)}{R_d T_a(0.622 + r_w)} \tag{A7}$$

where

$$r_w = 0.01Ue_{sat}(T_a)0.622p_a^{-1} \tag{A8}$$

is the mixing ratio. The turbulent exchange coefficients c_H and c_E are computed according to *Kondo* [1975]. They can be written as

$$c_H = 1.3 \cdot 10^{-3} f\left(S_p\right) \tag{A9}$$

$$c_E = 1.5 \cdot 10^{-3} f\left(S_p\right) \tag{A10}$$

where S_p is the stability parameter defined as

$$S_p = \frac{s|s|}{|s| + 0.01} \tag{A11}$$

with

$$s = (T_s - T_a)w^{-2} \tag{A12}$$

[50] The expressions for $f(S_p)$ are the following:

$$\begin{aligned} &f\left(S_p\right) = 0 && \text{for } S_p \le -3.3 \\ &f\left(S_p\right) = 0.1 + 0.03S_p + 0.9\exp\left(4.8S_p\right) && \text{for } -3.3 < S_p < 0 \\ &f\left(S_p\right) = 1.0 + 0.63S_p^{1/2} && \text{for } S_p \ge 0 \end{aligned} \tag{A13}$$

[51] The latent heat of vaporization is computed as in *Gill* [1982]:

$$L(T) = 2.5008 \cdot 10^6 - 2.3 \cdot 10^3(T - 273.15) \tag{A14}$$

which allows us to estimate the evaporation rate E as

$$E = Q_E/L(T_s) \tag{A15}$$

Appendix B: Heat Flux Error Estimates

[52] In order to estimate the errors on the heat fluxes, the procedure described in *Artegiani et al*. [1997] is here summarized. Let Q be a heat flux component, a function of n parameters with mean values x_k ($k = 1, \ldots, n$) (the hourly values) and errors ε_k (the absolute hourly errors) or η_k (the relative hourly errors) (see section 2.2). We first calculate the "central" value Q using x_k, then n values Q_k^- using $x_k - \varepsilon_k$ or $x_k(1 - \eta_k)$ and n values Q_k^+ using $x_k + \varepsilon_k$ or $x_k(1 + \eta_k)$. The error on the heat flux component produced by the error on parameter k is given by

$$\delta_k = \left(|Q - Q_k^+| + |Q - Q_k^-|\right)/2 \tag{B1}$$

[53] The overall error E on Q is then estimated by combining δ_k quadratically:

$$E = \frac{1}{n}\left(\sum\nolimits_k \delta_k^2\right)^{\frac{1}{2}} \tag{B2}$$

[54] **Acknowledgments.** F.R., C.C., and R.R.C. gratefully acknowledge the partial support of EU FP7 project JERICO, under grant 262584, and of the National Research Council Operational Planning Office (CNR-

UPO). V.M. and B.C. are indebted to the group performing the national monitoring program (under the EU Water Framework Directive), funded by the Slovenian Agency of Environment, and to the research program funded by the Ministry of Higher Education and Technology of Slovenia (contract P1–0237). M.C., D.G., and A.P. are indebted to the marine coastal waters monitoring program of the Friuli Venezia Giulia Region under EU Water Framework Directive 2000/60/CE and D.M. 260/10. The technical staff of CNR-ISMAR, NIB-MBS, ARPA FVG, and INOGS are gratefully acknowledged by the authors for operating and maintaining the stations and collaborating in the periodic surveys in the Gulf of Trieste.

References

Artegiani, A., D. Bregant, E. Paschini, N. Pinardi, F. Raicich, F., and A. Russo (1997), The Adriatic Sea general circulation. Part I: air-sea interactions and water mass structure, *J. Phys. Oceanogr.*, *27*, 1492–1514, doi:10.1175/1520-0485(1997)027<1492:TASGCP>2.0.CO;2.

Castellari, S., N. Pinardi, and K. Leaman (1998), A model study of air–sea interactions in the Mediterranean Sea, *J. Mar. Syst.*, *18*, 89–114.

Cozzi, S., M. Giani, C. F. Falconi, C. Comici, V. Turk, B. Čermelj, and N. Kovac (2012), Recent evolution of river discharges in the Gulf of Trieste (Northern Adriatic Sea) and their potential responses to anthropogenic pressure and climate changes, *Estuar. Coast. Shelf Sci.*, *115*, 14–24, doi:10.1016/j.ecss.2012.03.005.

Crisciani F., and F. Raicich (1999), Time variability of atmospheric and marine parameters over the Adriatic region, *N. Cim. C*, *22*, 181–189.

Crisciani, F., and F. Raicich (2004), A minimal model of adiabatic isotherms surfacing in very shallow waters, *Environ. Fluid Mech.*, *4*, 113–125.

Crise, A., S. Querin, and V. Malačič (2006), A strong bora event in the Gulf of Trieste: a numerical study of wind driven circulation in stratified conditions with a preoperational model, *Acta Adriatica*, *47*(Suppl.), 185–206.

Dorman, C. E., et al. (2006), February 2003 marine atmospheric conditions and the bora over the northern Adriatic, *J. Geophys. Res.*, *111*, C03S03, doi:10.1029/2005JC003134.

Fofonoff, N. P. (1985), Physical properties of seawater: A new salinity scale and equation of state of seawater, *J. Geophys. Res.*, *90*(C2), 3332–3342, doi:10.1029/JC090iC02p03332.

Gill, A. E. (1982), *Atmosphere–Ocean Dynamics, International Geophysics Series*, vol. 30, Academic, New York.

Kondo, J. (1975), Air–sea bulk transfer coefficients in diabatic conditions, *Boundary-Layer Meteorol.*, *9*, 91–112.

Malačič, V., and B. Petelin (2001). Gulf of Trieste, in *Physical Oceanography of the Adriatic Sea. Past, Present and Future*, edited by B. Cushman-Roisin, M. Gačić, P.-M. Poulain, and A. Artegiani, pp. 167–181, Kluwer Acad., Dordrecht.

Malačič, V., M. Celio, B. Čermelj, A. Bussani, and C. Comici (2006), Interannual evolution of seasonal thermohaline properties in the Gulf of Trieste (northern Adriatic) 1991–2003, *J. Geophys. Res.*, *111*, C08009, doi:10.1029/2005JC003267.

Mihanović, H., et al. (2013), Exceptional dense water formation on the Adriatic shelf in the winter of 2012, *Ocean Sci.*, *9*, 561–572, doi:10.5194/os-9–561-2013.

Payne, R. E. (1972), Albedo of the sea surface, *J. Atmos. Sci.*, *29*, 959–970, doi:10.1175/1520-0469(1972)029<0959:AOTSS>2.0.CO;2.

Picco, P. (1991), Evaporation and heat exchanges between the sea and the atmosphere in the Gulf of Trieste during 1988, *N. Cim. C*, *14*, 335–345.

Press, W. H., S. A. Teutolsky, W. T. Vetterling, and B. P. Flannery (1996), *Numerical Recipes in Fortran 77*, vol. *1*. Cambridge Univ. Press, Cambridge, USA.

Rinaldi, A. (2006), Stima dei forzanti atmosferici per la determinazione dei flussi di calore all'interfaccia aria-mare [in Italian], Laurea Magistrale thesis, Fac. of Eng., Univ. of Trieste, Trieste, Italy.

Simpson, J. J., and C. A. Paulson (1979), Mid-ocean observations of atmosphere radiation, *Q. J. R. Meteorol. Soc.*, *105*, 487–502.

Stravisi, F., and F. Crisciani (1986), Estimation of surface heat and buoyancy fluxes in the Gulf of Trieste by means of bulk formulas, *Boll. Oceanol. Teor. Appl.*, *4*, 55–61.

Supić, N., and M. Orlić (1999), Seasonal and interannual variability of the northern Adriatic surface fluxes, *J. Mar. Syst.*, *20*, 205–229.

Vatova, A. (1934), L'anormale regime fisico-chimico dell'Alto Adriatico nel 1929 e le sue ripercussioni sulla fauna [in Italian], *Thalassia*, *1*(8), 1–49.

World Meteorological Organization (1983), *Guide to Meteorological Instruments and Methods of Observation*, 5th ed., Rep. 6.7-6, Geneva.